ELSEVIER

Journal of Organometallic Chemistry 556 (1998) 11–20

Journal of Organometallic Chemistry

Ferrocenic acid derivatives: towards rationalizing changes in the electronic and geometric structures

Lily Lin, Attila Berces, Heinz-Bernhard Kraatz *

NRC-Steacie Institute for Molecular Sciences, 100 Sussex Drive, Ottawa, ON K1A 0R6, Canada

Received 8 July 1997; received in revised form 24 November 1997

Abstract

Using calculations based on Density functional theory (DFT), we optimized the geometry of three compounds containing the ferrocenoyl moiety, ferrocene aldehyde (**I**), ferrocene carboxylic acid (**II**), ferrocene amide (**III**) and the parent ferrocene. The calculated results were compared to experimental structural data. General trends have emerged: the carbonyl C–O distance increases in the order aldehyde < ketones < amides < acid. The O–C–X (X = O, N, C) angles are less responsive to substituents and seem to be more a reflection of packing forces. Expectedly the distance between carbonyl carbon and the organic group R (R=OH (acid), NR_2 (amide), CR_3 (ketone) increases in the order acid < amides < ketones. Maximization of electron delocalization involving the C(O)–X (X = O, N, C) and the Cp ring will force the Cp ring and the C(O)–X substituent to be co-planar. However, steric interference between the Cp ring and the substituent can result in a significant deviation from co-planarity and can give rise to a significant twist.

Keywords: Ferrocene; Ammonium ion; Electronic and geometric structures

1. Introduction

In view of the increasing importance of ferrocenes in asymmetric catalysis [1] and enantioselective synthesis [2] there has been renewed interest in the synthesis and chemistry of substituted ferrocenes [3]. Ferrocene-based systems are widely used as redox sensors. Beer's ammonium ion redox-responsive receptor utilizes a ferrocene moiety as a simple redox sensor to monitor substrate binding [4]. Ferrocene moieties have been incorporated into large proteins to act as redox relays [5]. Amide bond formation between the ferrocene carboxylic acid and the amine-sidechain of lysine is particularly convenient for protein labelling. We have recently reported a simple synthetic strategy for the formation of ferrocenoyl amino acids [6], allowing the N-terminal incorporation of a redox moiety into larger peptide assemblies. Ferrocenes exhibit a well-characterized one-electron reversible oxidation wave. Both, ferrocene and ferricenium cation are stable under a wide range of experimental conditions making ferrocene and its derivatives extremely useful as an electrochemical probe [7]. Substituents will influence the redox behavior of the ferrocene moiety by changing the energy level of the HOMO [8].

In accord with theoretical and experimental results, an electron withdrawing acyl group lowers the energy level of the highest occupied molecular orbital (HOMO), making it more difficult to oxidize [8]. For example, a coplanar arrangement of a phenyl-ring or carbonyl groups attached to the Cp ring of the ferrocene moiety, should allow for maximum interaction of the two π-systems and transmittance of ligand influences. Any deviations (e.g. due to sterics) from coplanarity will influence the electronic interaction between the two π-systems.

In this paper, we are particularly interested in understanding possible electronic factors leading to structural distortions of the ferrocenoyl group. In order to investi-

* Corresponding author. Present address: Department of Chemistry, University of Saskatchewan, 110 Science Place, Saskatoon, SK S7N 5C9, Canada; fax: +1 613 9914278; e-mail: kraatz@skvwav.usask.ca

0022-328X/98/$19.00
PII S0022-328X(97)00785-7

Table 1
Selected structural parameters of ferrocenoyl compounds

Entry	d(C=O)	d(C–C(0))	<(O–C–E)	Cp-bent	Cp/COR angle	Ref.
1	1.261(15)	1.407 (15)	121.24(11)	coplanar		[10]
1	1.232(2)	1.462(2)	123.15(13)	coplanar		this work
2	1.268(10)		123(1)	coplanar	0.5/4.1	[11]
2	1.233(3)	1.468 (3)	123.6(3)	3.1 (278K)		[12]
3	1.228(5)		123.5(5)			[13]
4	1.200(4)		124.3(3)			[13]
5	1.243(7)		123.5(5)	2.5/3.2	11.6/5.0	[14]
6a	1.258(5)		122.1(6)	2.6	19.8	[14]
6b	1.245(9)	1.476(9)	121.7(6)			[15]
6c	1.248(8)	1.468(7)	122.1(4)			[15]
6d	1.273(12)	1.473(19)	122.5(12)			[15]
7	1.244(12)	1.462(14)	126.0(8)	3.65(ecl)	14.39	[16]
8	1.200(5)	1.473(6)	123.2(5)		15.6/6.0	[17]
9	1.241(11)	1.507(12)	122.3(8)	1.3	16.7	this work
10	1.222(18)	1.472(19)	120.4(12)		15.7/50.2(!)	[18]
11	1.232(6)	1.501(7)	120.9(5)			[17]
12	1.235(4)	1.461(5)				[19]
13	1.219(4)	1.475(4)	121.5(3)			[20]
14	1.268(3)	1.471(4)	129.6(3)			[21]
15[a]	1.222(18)	1.472(19)	120.4(12)			[22]
16[a]	1.236(6)	1.499(7)	122.5(4)		14.1	[6]
17[a]	1.21(2)	1.43(2)	123.6(26)	1.8	5.4	[6]
18	1.242(2)	1.501(2)	120.6(2)	1.8	6.1	[23]
19	1.233(2)	1.504(3)	121.4(2)	2.8	24.1	[23]
20	1.238(3)	1.498(3)	121.0(2)	1.1	17.0	B.J. Chapel personal communication
21	1.047(11)	1.481(14)		0.9		[24]
22	1.203(7)	1.460(7)	118.3(5)		14.2	[25]a
23 ac	1.210(6)	1.450(7)	120.5(5)			[26]
benz1.	1.217(6)	1.474(7)	118.1(5)			
24	1.218	1.471	121.2	1.0		[27]

[a] Two molecules per asymmetric unit.

gate these effects in more detail and to possibly gain insight in the causes for the variations in electrochemical properties, we carried out electronic structure calculations based on gradient corrected density functional theory which has repeatedly shown to provide exceptionally accurate energetic and structural information for transition metal systems [9]. We optimized the geometry of three representative compounds containing the ferrocenoyl moiety, ferrocene aldehyde (**I**), ferrocene carboxylic acid (**II**), ferrocene amide (**III**) and the parent ferrocene.

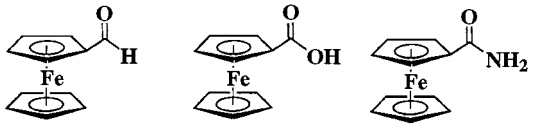

I II III

Due to our particular interest in ferrocene amides, we are focusing our discussions of electronic and geometric structures on ferrocene carboxylic acids and amides. In order to assess the significance of our calculation, we are presenting them in comparison to experimental structural data of known compounds containing the ferrocenoyl moiety.

2. Results and discussion

2.1. Geometric structure

2.1.1. Ferrocene carboxylic acids

We begin our discussion with the parent ferrocene carboxylic acids. The pertinent structural data for ferrocene carboxylic acids (entry **1**–**4**)

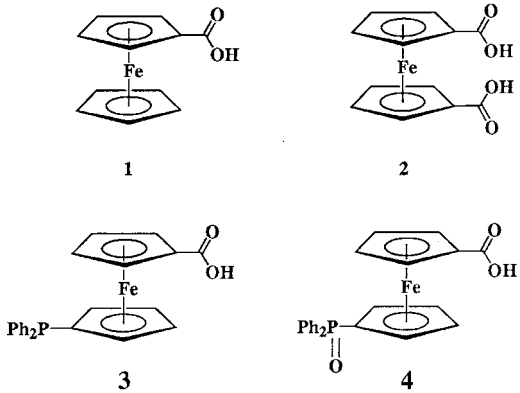

and some of their metal salts (entry **5**, **6a**–**7**) is summarized in Table 1. The structure of ferrocene carboxylic acid (**1**), determined by Cotton et al. [10]a, consists of

Table 2
Optimized geometries of substituted ferrocenes (all distances in Å and angles in °)

	Ferrocene	I	II	III
d(C–C)	1.432	1.429–1.440	1.425–1.442	1.425–1.444
d(C–Fe)	2.059	2.052–2.066	2.035–2.068	2.048–2.072
d(C=O)		1.220	1.221	1.266
d(C–C(X))		1.485	1.460	1.460
d(C–X)		1.120 (H)	1.376 (O)	1.463 (N)
α(O–C–X)		120.2	122.4	123.5
α(Cp–Fe–Cp)	180.0	178.4	177.4	178.4
τ(Cp/COX)		5.9	4.1	4.7

hydrogen-bonded dimers with Fe–C bond distances of 2.047 (14) Å for the substituted Cp ring and a Fe–C distance of 2.038 (14) Å for the unsubstituted Cp ring [10]. This compares well to simple ferrocene with a d(Fe–C) of 2.05 Å [28]. H-bonded dimers having similar structural features are obtained also for systems that carry substitutents at the opposite ring. 1-PPh_2-1′-COOH(Fc) (**3**), a centrosymmetric dimer, and 1-$P(O)Ph_2$-1′-COOH(Fc) (**4**) have their carboxyl groups in coplanar arrangement with the Cp rings. The Cp rings are parallel with a tilt of $< 3°$. **4** exhibits an interesting solid state arrangement in that it forms H-bonds between the phosphine oxide and the carboxylic OH group giving zigzag chains, with a O···O of 2.588 (3) Å [13].

Ferrocene-1,1′-dicarboxylic acid (**2**) crystallizes as O–H···O H-bonded dimers in two modifications. The monoclinic modification [11] exhibits a disorder showing the H-atom of the acid group equally distributed over two sites between the oxygens atoms of the dimeric unit. The triclinic modification [12] has well ordered positions for the acidic H-atom and well-defined C=O and C–O bonds (d(C=O) = 1.233 (3) and d(C–O) = 1.300 (3) Å). In both modifications, the two Cp rings of the ferrocene dicarboxylic acid moiety are almost eclipsed (twisted with respect to each other (1.4°) and deviate only slightly from co-planarity (bent of 1.2°). The O–C–O angle is opened up by ca. 2° as compared to the mono-carboxylic acid. The tilt between the Cp-plane and the carboxy-plane (0.5° and 4.1°) allows for efficient overlap of the two π-systems.

For comparative purposes, we have carried out a full geometry optimization of ferrocene carboxylic acid, $(C_5H_5)Fe(C_5H_4CO_2H)$ **II**. The results are summarized in Table 2 and Fig. 1. On first sight, the overall geometry is well reproduced. The Fe–C bond distances are well within the established Cp–Fe distances for other crystallographically determined ferrocene carboxylic acids (see Table 1 entry **1**–**4**). The carboxy-

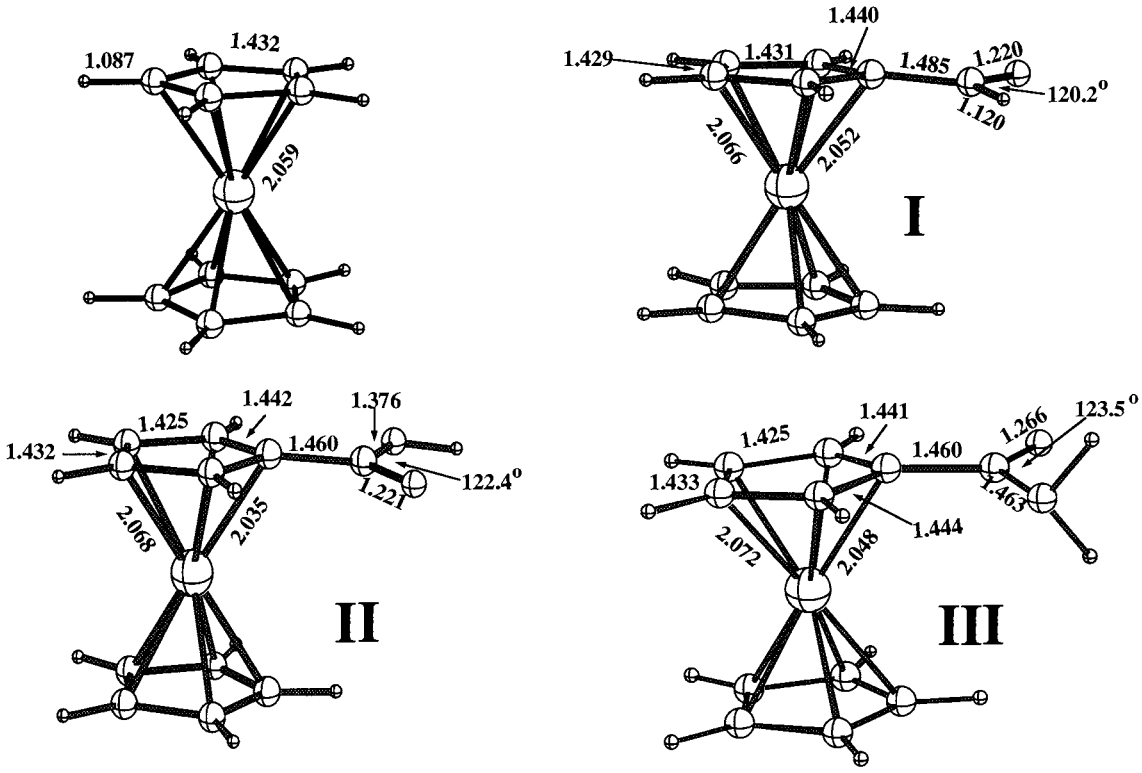

Fig. 1. Optimized geometries of ferrocene (top left), ferrocene aldehyde (**I**), ferrocene carboxylic acid (**II**), and ferrocene amide (**III**). Selected bond distances and angles are illustrated (also see Table 2).

group is almost co-planar with the Cp-ring to which it is attached (twist of 4.1°). Both Cp rings are nearly parallel to each other (Cp bent of 2.6°). However, there are noteworthy differences. The C–C(O) distance was calculated to be 1.460 Å. Interestingly, this is significant longer than the crystallographically determined bond distance for **1** (1.407 (15) Å), but compares well with that of 1,1′-ferrocene dicarboxylic acid and other ferrocene carboxylic acids [10,13,11,12]. We were surprised to find this discrepancy between our calculated C–C(O) distance and that measured by Cotton [10]a. Hence, we carried out a careful low temperature single crystal X-ray diffraction study of **1** (for a full analysis, see supplementary material) [29,30]. Our experimental results for the C–C(O) bond distance of 1.462(2) Å is in agreement with our theoretical findings [31].

Ferrocene carboxylates can act as ligands to metal ions. Coordination should be manifested in structural changes that express a change in electronic structure, such as a change in d(C=O) or change in the tilt of Cp versus carboxy-planes. Structural parameters of some ferrocene carboxylates are summarized in Table 1 (entry **5**, **6a**–**7**).

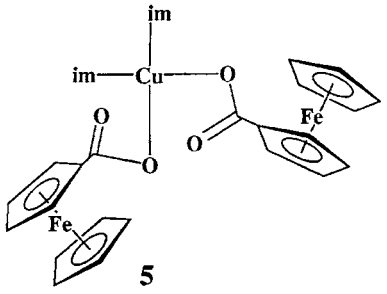

5

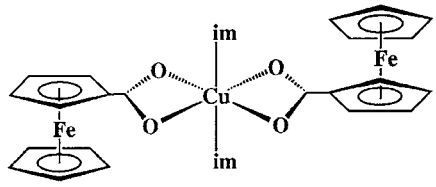

6

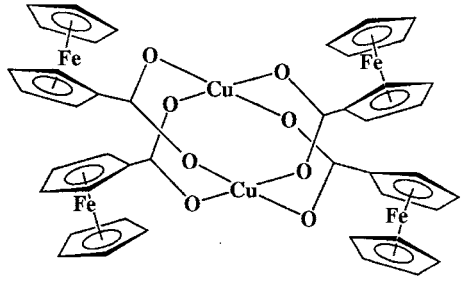

7

Whereas the dihedral angle between the Cp and the carboxy planes increase upon coordination of ferrocene carboxylate to various metals, there is no significant change in the Cp–C(O) separation. Furthermore, no changes of the O–C–O angle are observed, nor does metal coordination increase the C–O separation. Coordination of **1** to Cu^{2+} causes only a small shift to higher energy in the Vis absorption from 460 nm in free ferrocene carboxylic acid to 458 nm in **6b**, **6c** and 455 nm in **5**, **6a** and **6d** [14–16]. Electrochemical studies on these systems support the UV studies in that the 1-e oxidation wave of the ferrocene/ferrocenium couple is virtually unaffected by Cu coordination, suggesting that the ferrocene orbitals are only slightly disturbed by metal coordination. This is in accord with theoretical considerations suggesting that a one-electron oxidation will be Fe-based. Although the highest molecular orbital (HOMO) will be influenced by the carboxylate substituent, more remote changes (such as Cu coordination) are not expected to result in a great variation of the HOMO energy. Hence it does not seem surprising that no change in redox behavior was observed.

2.1.2. Ferrocene amides

Fig. 1 and Table 2 summarize the pertinent structural features of the optimized structure of ferrocene amide, $(C_5H_5)Fe(C_5H_4CONH_2)$ **III**. As expected, both Cp rings are nearly parallel (Cp bent angle 1.6°). Both amide and Cp planes are close to co-planar with a negligible twist of 4.7°. The C–C(O) distance of **III** is identical to that of **II**. Upon amidation the Fe–C(Cp) distances and the C=O distances (from 1.221 Å in **II** to 1.266 Å in **III**) increase. The C=O bond distances of structurally characterized ferrocene amides are between 1.20 and 1.26 Å (see Table 1) and seem to be related to steric factors or packing forces rather than electronic factors. The calculated C(O)–N distance of 1.463 Å is significantly larger than those observed for a series of ferrocene amides, which fall in the narrow range of

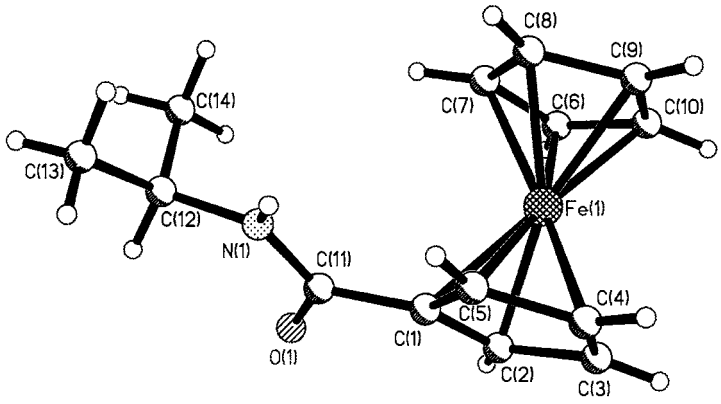

Fig. 2. Structural representation of FcNH^{i}Pr (**9**). Selected bond lengths and angles: C(1)–C(11) = 1.507(12) Å, C(11)–O(1) = 1.241(11) Å, N(1)–C(12) = 1.462(12) Å, O(1)–C(11)–N(1) = 122.3(8)°, C(11)–N(1)–C(12) = 121.5(8)°.

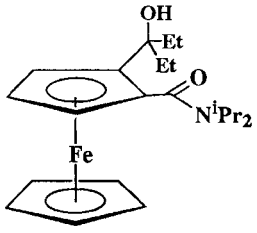

18

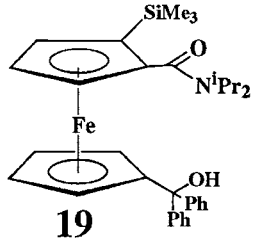

19

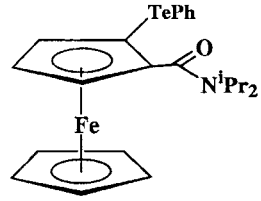

20

1.330(4)–1.368(4) Å (see Table 1). However, extreme ring-strain, such as observed in Hirao's macrocyclic 2-pyridyl-1,1′-ferrocenedicarboximide will lead to an elongation of the C(O)–N bond (1.446 (8) and 1.408 (8) Å) [32].

The structural data for some ferrocene amides is summarized in Table 1. In absence of any ring strain, a simple 1,3′-amide such as **8** exhibit a coplanar arrangement of the amide groups and the Cp ring [19]. In light of a dearth of structural information on simple monosubstituted ferrocenoyl amides, we decided to carry out a single X-ray study of FcC(O)NH(^{i}Pr) (**9**) [33,34], first prepared by Beer et al. [4].

The structure of FcC(O)NH(^{i}Pr) is shown in Fig. 2. **9** crystallizes in the monoclinic space group $P2_1/c$. The Cp rings are parallel to each other (Cp bent angle 1.3°). The Cp–C(O) distance of 1.507(12) Å is within the range of other simple ferrocenoyl amides, such as ferrocenoyl glutamyl dibenzyl ester (**16**) [6] (1.499(7) Å and 1.507(7) Å) and ferrocenoyl cysteinyl(S-benzyl) methylester (**17**) [6] (1.43(2) Å and 1.48(2) Å) and others (**18**–**20**).

The amide group C(O)–N is planar and exhibits common C–N and C–O bond distances and angles. It is rotated with respect to the Cp plane by 16.7°. The isopropyl substituent is rotated by 104.6° with respect to the amide plane, most likely due to a minimization of steric interaction between the bulky isopropyl substituent on the amide nitrogen and the Cp ring. Similar steric effects have been observed for benzoyl ferrocene (vide infra). In addition, **9** exhibits extensive hydrogen bonding between the amide N–H and the carbonyl oxygen of an adjacent molecules (d(O···N) = 2.95 Å), forming an infinite chain.

In macrocyclic systems, such as **10**, ring strain can lead to extensive distortion from planarity, causing a rotation of the Cp and amide planes of 50.2°, with respect to each other [18]. In Hirao's imide [3] ferrocenophane, the Cp/amide rotations are 34.6° and 45.7°

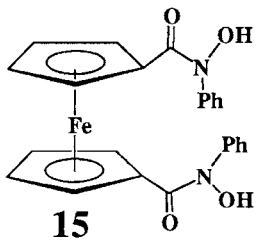

15

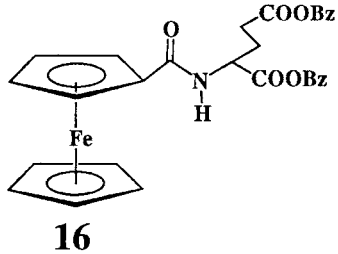

16

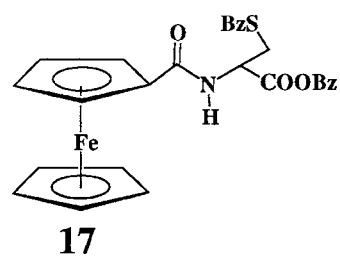

17

for the two amide groups [32]. In addition, the complex exhibits an unusually large Cp bending angle of 16.4°! In other mono-amides (**19**–**21**), only moderate twists up to 24.1° (for **20**) are observed, most likely due to steric interactions between the Cp ring and the substituent on the amide. Although a coplanar arrangement will allow for maximum π-orbital overlap between the Cp and amide π-systems, an angle between Cp and amide planes of 30° will decrease the orbital interaction by only ca. 14% and even a twist of 50.2°, as in the case for **9**, will still allow for ca. 60% of the orbital interaction ($\cos\theta$–relationship)! We have estimated the barrier for rotation of the amide group about the C–C(O) bond to be about 35–40 kJ mol^{-1} (estimated as the difference of the total bond energies of **II** in C_s and C_1 geometry). In general, ring strain causes the d(C–N) to be elongated with respect to the simple amide **8**, giving it more single bond character.

Experiments show that in the absence of strong intermolecular forces, such as hydrogen bonding (see 1,1′-ferrocene dicarboxylic acid, vide supra) [11,12], most of the disubstituted systems crystallize in the 1,3′ conformation (e.g. **8**). This is not too surprising, since this configuration minimizes the steric repulsion between the groups and still allows an eclipsed conformation of the Cp rings. If the two substituents are tied together as part of a macrocyclic system (**10** and **11**), the ferrocene system adopts a 1,2′ conformation due to

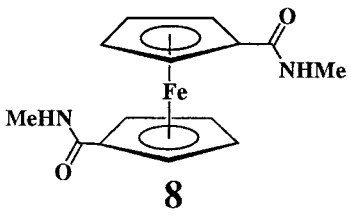

8

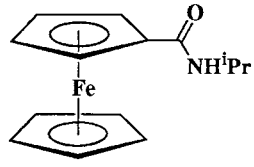

9

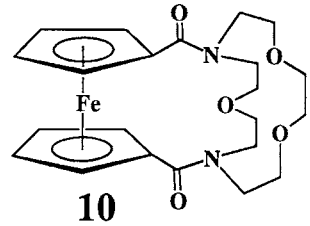

10

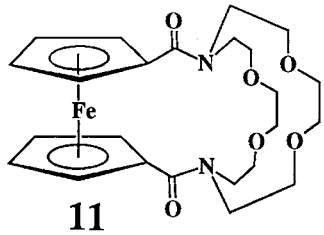

11

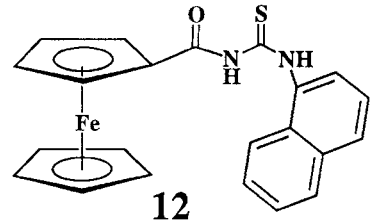

12

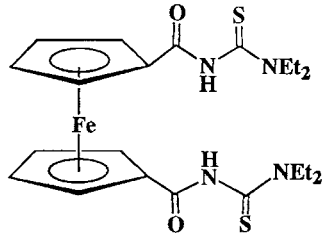

13

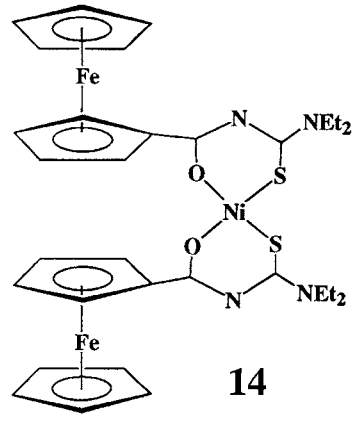

14

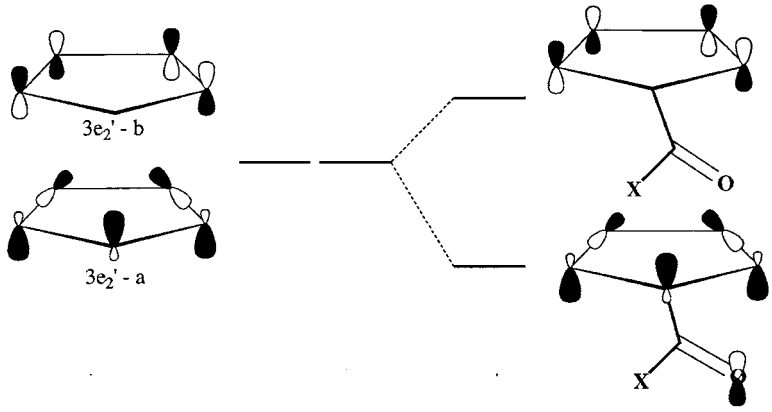

Scheme 1. The interaction pattern of the HOMO of ferrocene with the substituent orbitals.

the geometric requirements imposed by the macrocycle. Similar geometries have been observed for ferrocenophanes [17].

Ferrocenoyl acetylthioureas, generally obtained by reaction of ferrocenoyl chloride with KSCN, followed by the reaction with primary amines, form an interesting class of compounds in that they can act as bidentate *O*,*S*-ligands to metal centers. Bond distances and angles are similar to those of simple ferrocenoyl amides (see Table 1 entry **12**–**14**). Hydrogen abstraction leads to an anionic ligand able to coordinate to transition metal ions in a bidentate fashion. Expectedly, coordination has structural consequences. For example, coordination of the ferrocenoyl acetylthiourea ligand to Ni^{2+} results in elongation of the C=O bond by about 50 pm and a shortening of the C–N bond by about 35 pm. In addition, the O–C–N angle is significantly larger (129.6 (3)° (complexed) as compared to 121.5 (3)° (uncomplexed)).

2.1.3. Ferrocene ketones

For completion, we wish to include a short section on ferrocene ketones. Fig. 1 and Table 2 summarize the important features of the geometry optimization of $(C_5H_5)Fe(C_5H_4CHO)$ (**I**, **21**). The overall calculated structure is in good agreement with the experiment [24]. The two Cp rings are virtually parallel (Cp bent angle calc. 1.6°; exp. 0.9°) and eclipsed. The –CHO group is almost coplanar with the Cp ring to which it is attached (twist calc. 5.9°, exp. 6.2°). This arrangement allows for conjugation between the Cp ring and the –CHO group. The Cp–CO bond distance confirms conjugation and is between that of a single and double bond (d(C–C) calc. 1.485 Å; exp. 1.481 (14) Å). It is noteworthy that the agreement between experiment and calculation is less accurate for the C=O bond length (d(C=O) calc. 1.220 Å; exp. 1.047 (11) Å). The structural features of other ferrocene ketones is summarized in Table 1 (entry **21**–**24**).

Similarly to other ferrocenoyl complexes, benzoyl ferrocene (**22**) [25]a exhibits signs of double bond localization in the substituted Cp ring. This effect is also evident from the short Cp–CO distance of 1.467 (3) Å as compared to the Ph–CO of 1.496 (3) Å. The amide plane is slightly rotated out of the Cp plane by 14.2°.

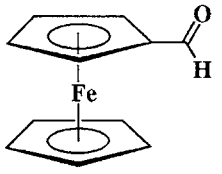

21

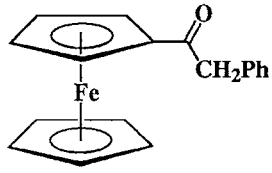

22

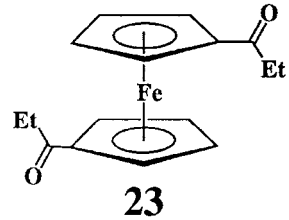

23

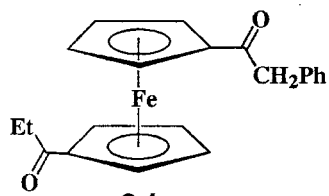

24

Probably due to steric interference between the phenyl and the Cp groups, the phenyl substituent is rotated out of the Cp plane by 40.4°. Another structure determination under similar conditions gives similar results having a a short Cp–CO bond (1.460 (7) Å) and an elongated Ph–CO bond (1.491 (8) Å) [25]b.

1-Acetyl-1′-benzoyl ferrocene (**23**) is an interesting case, since it has both the acetyl and benzoyl group attached to the Cp rings. Hence it allows a direct comparison of the relative influence of the other substituent with respect to changes in bond distances and angles in the other substituent. The molecule adopts a 1,3′ configuration, familiar for disubstituted ferrocenes. For the 1-benzoyl substituted Cp ring, the Cp–CO (1.474 (7) Å and CO–Ph (1.498 (7) Å) bond distances are almost identical to simple benzoyl ferrocene 1.474 (7) Å. The benzoyl group is rotated out of the Cp plane by 43.57°. The Cp–CO distance for the 1′-acetyl group is significantly shorter (1.450 (7) Å) indicating it having more double bond character (C–C is 1.54 Å and C=C is 1.40 Å). The acetyl group is nearly co-planar with the Cp ring to which it is attached, allowing for an ideal interaction between the π-systems [26].

In contrast, the acetyl groups in 1,3′-diacetyl-Fc [27] are twisted out of the Cp planes by 11.1 and 8.48°, respectively. The elongation of the Cp–CO distance to 1.474 (7) and 1.468 (7) Å is most likely due to the effect of the substituent on the other Cp ring. It seems that the presence of CO–R group in which R can be involved in electron-delocalization leads to a shortening of the Cp–CO bond on the other ring.

3. Electronic structure

The electronic structure of ferrocene has been extensively studied and became a textbook example for the bonding in MCp and MCp_2 systems [35]. To interpret the trends in the structural, spectral, chemical and electrochemical properties of substituted ferrocenes it is of interest to study the effect of ligand substitution on the molecular orbitals, especially on the higher lying occupied orbitals. The HOMO of ferrocene is an essentially non-bonding metal based orbital of e_2' symmetry, which correlates to the x^2-y^2 and xy orbitals of iron in standard orientation. An iron based z^2 orbital is below the HOMO of ferrocene followed by two degenerate pairs of bonding orbitals between the π system of the Cp ring and the iron d orbitals. These π orbitals play an important role in substituted ferrocenes since the π system can extend to the substituents. The ligands considered in this study are all electron withdrawing by accepting electrons in the unoccupied π^* orbitals.

One important effect of ligand substitution is the splitting between the two components of the degenerate ferrocene orbitals. Usually, one of the two components of the degenerate orbitals have the proper nodal characteristics to interact with the ligand based orbitals while the other is non-interacting. We demonstrate this effect by considering the two components of the HOMO of ferrocene. These are both metal based orbitals, but the ligand contribution is different in the substituted systems compared to ferrocene. To show the differences, we consider the ligand contribution only to these orbitals. In the aldehyde, acid, and amide derivatives the two orbitals which correspond to the $3e_2'$ of ferrocene are separated by 0.046, 0.082 and 0.065 eV, respectively. Other degenerate orbitals which are Cp-based are split even more. For each substituted ferrocene the 'a' component of the $3e_2'$ is stabilized and the 'b' component is not interacting with the substituents and becomes the HOMO of the substituted system. Scheme 1 illustrates the general interaction pattern of the HOMO of ferrocene with the substituent orbitals. The 'b' component of the ferrocene HOMO orbital has almost zero contribution from the C_1 carbon atom, which makes this orbital less capable to overlap with the ligand based orbitals. The 'a' component (see Scheme 1), however, has a significant contribution from C_1 carbon, hence has some overlap with the orbitals of the substituents. The 'a' component of ferrocene HOMO is stabilized by a contribution from the carbonyl oxygen p_π orbital, which is a general pattern for all systems.

In addition to the metal based HOMO orbitals, the Cp based p orbitals also play a significant role in the in the electronic structure of substituted ferrocene. Some of the structural differences between the acid and amide derivatives of ferrocene originate from the differences in the electronic structure of substituents. The π type orbitals of the substituents can interact with the π system of the Cp ring on ferrocene. The LUMO of both the amide and the acid are antibonding π orbitals (Scheme 2) between the C–O and C–X (X = O, N) atom pairs which interact with the occupied π orbitals of the Cp ring on ferrocene. The LUMO of the amide is lower in energy than that of the acid making the amide slightly more electron withdrawing. The highest occupied π type orbitals of the amide and the acid also interact with the ferrocene. In this respect there is an important difference between the acid and the amide:

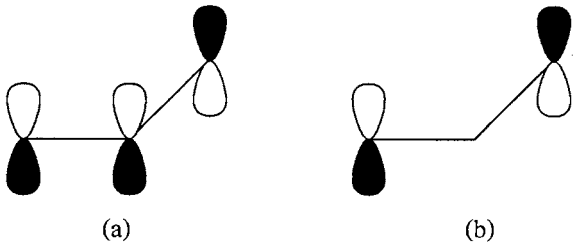

Scheme 2. The LUMO of both the amide and acid groups.

the highest π type orbitals of the acid is non-bonding while that of the amide is bonding between the carbonyl C and O atoms. The withdrawal of electron density from the highest π type orbital thus leads to weakening and lengthening of the CO bond in the amide more than in the acid.

4. Computational details

The reported calculations were carried out with the Amsterdam Density Functional (ADF) program system version 2.0.1 derived from the work of Baerends et al. [36] and developed at the Free University of Amsterdam [37] and at the University of Calgary [38]. All optimized geometries calculated in this study are based on the local density approximation [39] (LDA) augmented with gradient corrections to the exchange [39]b and correlation [39]c potentials. These optimizations were carried out by the direct inversion of iterative subspace for geometry (GDIIS) technique [40] with natural internal coordinates [41]. We have combined the ADF program with the GDIIS program [42] and previously implemented the skeletal internal coordinates [43]. The internal coordinates were generated by the INTC program [44] and augmented by hand.

The atomic orbitals on iron were described by an uncontracted triple-ζ STO basis set [45], while a double-ζ STO basis set was used for carbon, nitrogen, oxygen and hydrogen; a single-ζ polarization function was used on all atoms. The $1s^2$ configuration on carbon, nitrogen and oxygen as well as the $1s^22s^22p^6$ configuration of iron were assigned to the core and treated by the frozen-core approximation [38]. A set of auxiliary s, p, d, f, g and h STO functions, centred on all nuclei, was used in order to fit the molecular density and represent the Coulomb and exchange potentials accurately in each SCF cycle [46].

The numerical integration accuracy parameter which approximately represents the number of significant digits for the scalar matrix elements was gradually increased to 4.5 until convergence with respect to integration accuracy was reached. This numerical accuracy is sufficient to determine energies within a fraction of a kJ mol^{-1}, and bond distances within 0.001 Å (which is more accurate than predicted by the numerical integration accuracy parameter).

5. Summary

Despite the multitude of chemical variety of ferrocenoyl compounds having the chemical formula $(C_5H_5)Fe(C_5H_4C(O)X)$, there is surprisingly small structural variation with the chemical nature of substituent X. It is obvious from Table 1 that a trend exists for d(C=O), with d(C=O) of aldehyde < ketones < amides < acid. The O–C–X (X = O, N, C) angles are less responsive to substituents and seem to be more a reflection of packing forces. In addition, d(C(O)–O) < d(C(O)–N) < d(C–C). Amides show a narrow range of C(O)–N distances between 1.330 (4) and 1.368 (4) Å. Maximization of electron delocalization involving the C(O)–X (X = O, N, C) and the Cp ring will force the Cp ring and the C(O)–X substituent to be co-planar. However, steric interference allows for a significant deviation from co-planarity. Large substituents on the C(O)–X group can give rise to a significant twist. Likewise ferrocene cyclophanes exhibit larger twists than comparable open systems. As pointed out, orbital interaction between the π-systems is still operational even at large twists of 40–50°. Hence, it can be concluded that this twist is most likely a reflection of crystal packing forces. All Cp–CO distances show significant double bond character. As was pointed out by Palenik, the eclisped conformation of the Cp rings is preferred in the absence of steric contraints and disorder of the molecules in the crystal state. Using calculations based on density functional theory, we optimized the structures of ferrocene aldehyde, ferrocene carboxylic acid and ferrocene amide. The geometries compare favorably with experimental data. Although our results suggest that one may predict structural trends semiquantitatively, our calculations also showed the complexity of the problem, which makes it very difficult to predict a priory quantitative trends without detailed calculations.

Acknowledgements

A. Berces is a Canadian Government Laboratory visiting fellow (1995–1997). H.-B. Kraatz is the recipient of an NRC research associateship (1996–1998). We thank Garry E. Enright for help with the X-ray data collections and Prof. Peter Pulay for providing the INTC program, used to generate the input for natural coordinate optimization.

References

[1] (a) A. Togni, T. Hayashi, Eds., Ferrocenes: Homogeneous Catalysis, Organic Synthesis, Material Science, VCH, Weinheim, 1995. (b) M. Sawamura, Y. Ito, Chem. Rev. 92 (1992) 857.
[2] G. Nicolosi, A. Patti, R. Morrone, M. Piatelli, Tetrahedron: Asymmetry 5 (1994) 1639.
[3] (a) T. Sammakia, H.A. Latham, D.R. Schaad, J. Org. Chem. 60 (1995) 10–11. (b) M. Tsukazaki, M. Tinkl, A. Roglans, B.J. Chapell, N.J. Taylor, V. Sniekus, J. Am. Chem. Soc. 118 (1996) 685–686.
[4] P.D. Beer, D.B. Crowe, M.I. Ogden, M.G.B. Drew, B. Main J.C.S., Dalton Trans. (1993) 2107–2116.

[5] (a) Y. Degani, A. Heller, J. Phys. Chem. 91 (1987) 1285–1289. (b) A. Heller, Acc. Chem. Res. 23 (1990) 128–134.
[6] H.B. Kraatz, J. Lusztyk, G.D. Enright, Inorg. Chem. 36 (1997) 2400–2405.
[7] see for example: (a) L. Zhang, L.A. Godinez, T. Lu, G.W. Gokel, A.E. Kaifer, Angew. Chem. Int. Ed. Engl. 34 (1995) 235–237. (b) C.E.D. Chidsey, C.R. Bertozzi, T.M. Putvinski, A.M. Mujsce, J. Am. Chem. Soc. 112 (1990) 4301–4306. (c) A. Badia, R. Carlini, A. Fernandez, F. Battaglini, S.R. Mikkelsen, A.M. English, J. Am. Chem. Soc. 115 (1993) 7053–7060.
[8] J.C. Green, Struct. Bond. 43 (1981) 37–112.
[9] (a) T. Ziegler, Chem. Rev. 91 (1991) 651. (b) A. Bérces, T. Ziegler, L. Fan, J. Phys. Chem. 98 (1994) 1584–1595.
[10] (a) F.A. Cotton, A.H. Reid, Jr., Acta Cryst. C 41 (1985) 686–688. (b) K. Iwai, M. Katada, I. Motoyama, H. Sano, Bull. Chem. Soc. Jpn. 60 (1987) 1961–1966.
[11] G.J. Palenik, Inorg. Chem. 8 (1969) 2744–2749.
[12] F. Takusagawa, T.F. Koetzle, Acta Cryst. B B35 (1979) 2888–2896.
[13] J. Podlaha, P. Stepnicka, J. Ludvik, I. Cisarova, Organometallics 15 (1996) 543–550.
[14] A.L. Abuhijleh, C. Woods, J. Chem. Soc. Dalton Trans. (1992) 1249–1252.
[15] A.L. Abuhijleh, J. Pollitte, C. Woods, Inorg. Chim. Acta 215 (1994) 131–137.
[16] M.R. Churchill, Y.-J. Li, D. Nalewajek, P.M. Schaber, J. Dorfman, Inorg. Chem. 24 (1985) 2684–2687.
[17] M.C. Grossel, M.R. Goldspink, J.A. Hriljiac, S.C. Weston, Organometallics 10 (1991) 851–860.
[18] C.D. Hall, I.P. Danks, S.C. Nyburg, A.W. Parkins, N.W. Sharpe, Organometallics 9 (1990) 1602–1607.
[19] J.-T. Wang, Y.-F. Yuan, Y.-M. Xu, Y.-W. Zhang, R.-J. Wang, H.-G. Wang, J. Organomet. Chem. 481 (1994) 211–216.
[20] O. Seidelmann, L. Beyer, G. Zdobinsky, R. Kirmse, F. Dietze, R. Richter, Z. Anorg. Allg. Chem. 622 (1996) 692–700.
[21] O. Seidelmann, L. Beyer, R. Richter, Z. Naturrforsch. B 50 (1995) 1684–1684.
[22] W. Zhang, F.-Z. Li, Q.-W. Liu, X.-Y. Huang, Jiegou Huaxue (Chin. J. Struct. Chem.) 14 (1995) 108–112.
[23] B.J. Chapell, V. Snieckus, J. Am. Chem. Soc. 118 (1996) 685–686.
[24] M.F. Daniel, A.J. Leadbetter, M.A. Mazid, J.C.S. Faraday Trans. 2 77 (1981) 1837–1849.
[25] (a) I.R. Butler, W.R. Cullen, S.J. Rettig, J. Trotter, Acta Cryst. C44 (1988) 1666–1667. (b) J.C. Barnes, W. Bell, C. Glidewell, R.A. Howie, J. Organomet. Chem. 385 (1990) 369–378.
[26] (a) G. Calvarin, J. Bouvaist, D. Weigel, C. R. Acad. Sci. Paris 268 (1969) 2288–2290. (b) P.G. Calvarin, D. Weigel, Acta Cryst. B27 (1971) 1253–1263.
[27] G. Palenik, Inorg. Chem. 9 (1970) 2429–2430.
[28] P. Seiler, J.D. Dunitz, Acta Cryst. B35 (1979) 2020.
[29] Crystal data for **1**: $C_{11}H_{10}FeO_2$, MW = 230.05, orange needles, crystal size = 0.30 × 0.15 × 0.15 mm, monoclinic space group $P2_1/n$, $a = 5.734(2)$ Å, $b = 12.782(3)$Å, $c = 12.550(3)$ Å, $\beta = 97.46(3)°$, $V = 912.0(5)$ Å^3, $Z = 4$, $D_{calc.} = 1.595$ g cm^{-1}, λ(Mo–K_α) = 0.71073 Å (graphite monochromated), $F(000) = 452$, $\mu = 1.613$ cm^{-1}, $R = 0.0226$ and $wR = 0.0574$ for $I > 2\sigma(I)$, $R = 0.0269$ and $wR = 0.0600$ for all data.
[30] Data collection was carried out on a Siemens SMART diffractometer equipped with a CCD collector. The structure was solved by direct methods and refined on F^2 data using the Siemens SHELXTL program system. All non hydrogen atoms were refined with anisotropic temperature factors. Hydrogen atoms were located in the density map and positions fully refined using isotropic temperature factors. The refinement converged at $R = 0.0226$, $wR = 0.0574$ (for all observed data $I > 2\sigma(I)$.
[31] According to our experimental findings, the structure of ferrocene carboxylic acid consists of hydrogen bonded acid dimers with d(O···O) = 2.656 Å, which is in good agreement with Cotton's structure (see ref. [11]a). In addition, we find a weak interaction of between the oxygen of the carboxylate with a C–H bond of the Cp of d(O···H) = 2.534 Å. This distance is clearly within the sum of the van der Waals radii and indicates a weak interaction.
[32] T. Moriuchi, I. Ikeda, T. Hirao, Organometallics 14 (1995) 3578–3580.
[33] Crystal data for FcC(O)NH(^{i}Pr): $C_{14}H_{17}FeNO$, MW = 271.14, thin yellow needles, crystal size = 0.45 × 0.05 × 0.02 mm, monoclinic space group $P2_1/c$, $a = 13.1973(10)$ Å, $b = 9.8447(8)$ Å, $c = 10.1206(8)$ Å, $\beta = 109.2590(10)°$, $V = 1241.3(2)$ Å^3, $Z = 4$, $D_{calc.} = 1.451$ g cm^{-1}, λ(Mo–K_α) = 0.71073 Å (graphite monochromated), $F(000) = 568$, $\mu = 1.197$ cm^{-1}, $R = 0.0979$ and $wR = 0.2300$ for $I > 2\sigma(I)$ ($R = 0.1474$ and $wR = 0.2724$ for all data). Due to the small crystal size only one quarter of all reflections were observed.
[34] Data collection was carried out on a Siemens SMART diffractometer equipped with a CCD collector. The structure was solved by direct methods and refined on F^2 using the Siemens SHELXTL program suite. All non-hydrogen atoms are refined anisotropically. Hydrogen atoms are placed in calculated positions (see supplementary material).
[35] T.A. Albright, J.K. Burdett, M.-H. Whangbo, Orbital Interactions in Chemistry, John Wiley and Sons, New York, 1985.
[36] E.J. Baerends, D.E. Ellis, P. Ros, Chem. Phys. 2 (1973) 41.
[37] (a) W. Ravenek, in: H.J.J. te Riele, Th. J. Dekker, H.A. van de Vorst (Eds.), Algorithms and Applications on Vector and Parallel Computers, Elsevier, Amsterdam, 1987. (b) P.M. Boerrigter, G. te Velde, E.J. Baerends, Int. J. Quantum Chem. 33 (1988) 87. (c) G. te Velde, Baerends, E.J., J. Comp. Phys. 99 (1992) 84.
[38] (a) L. Fan, T. Ziegler J. Chem. Phys. 94 (1991) 6057. (b) L. Fan, T. Ziegler, J. Chem. Phys. 95 (1991) 7401. (c) L. Fan, L. Versluis, T. Ziegler, E.J. Baerends, W. Ravenek, Int. J. Quantum Chem. S22 (1988) 173. (d) L. Fan, T. Ziegler, J. Chem. Phys. 96 (1992) 9005. (e) L. Fan, T. Ziegler, J. Phys. Chem. 96 (1992) 6937.
[39] (a) S.H. Vosko, L. Wilk, M. Nusair, Can. J. Phys. 58 (1980) 1200. (b) A.D. Becke, Phys. Rev. A 38 (1988) 2398. (c) J.P. Perdew, Phys. Rev. B 33 (1986) 8822. (d) J.P. Perdew, Phys. Rev. B34 (1986) 7046.
[40] (a) P. Császár, P. Pulay, J. Mol. Struct. 114 (1984) 31. (b) P. Pulay, Chem. Phys. Lett. 73 (1980) 393. (c). P. Pulay, J. Comput. Chem. 3 (1982) 556.
[41] (a) G. Fogarasi, X. Zhou, P.W. Taylor, P. Pulay, J. Am. Chem. Soc. 114 (1992) 8191. (b) P. Pulay, G. Fogarasi, F. Pang, J.E. Boggs, J. Am. Chem. Soc. 101 (1979) 2550.
[42] Programmed by A.G. Csaszar, P.G. Szalay, Eötvös University, Budapest, Hungary, 1984.
[43] (a) A. Bérces, J. Comp. Chem. 18 (1997) 45–55. (b) A. Bérces, T. Ziegler, J. Phys. Chem. 98 (1994) 13233. (c) A. Bérces, T. Ziegler, L. Fan, J. Phys. Chem. 98 (1994) 1584.
[44] INTC program to generate natural internal coordinates, P. Pulay, G. Fogarasi, 1992, Univerity of Arkansas, Fayetteville.
[45] (a) G.J. Snijders, E.J. Baerends, P. Vernooijs, At. Nucl. Data. Tables 26 (1982) 483. (b) P. Vernooijs, G.J. Snijders, E.J. Baerends, Slater Type Basis Functions for the whole Periodic System, Internal report, Free University of Amsterdam, The Netherlands, 1981.
[46] J. Krijn, E.J. Baerends, Fit functions in the HFS-method, Internal Report (in Dutch), Free University of Amsterdam, The Netherlands, 1984.